Available online at www.medicinescience.org

ORIGINAL ARTICLE

Medicine Science International Medical Journal

Medicine Science 2021;10(2):400-8

Synthesis, antimicrobial and in *silico* studies of new 2.5-disubstituted benzoxazole derivative

Meryem Erol[1], Ismail Celik[1], Gulcan Kuyucuklu[2]

[1]*Erciyes University, Faculty of Pharmacy, Department of Pharmaceutical Chemistry, Kayseri, Turkey*
[2]*Trakya University, Faculty of Medicine, Department of Medical Microbiology, Edirne, Turkey*

Received 14 October 2020; Accepted 02 December 2020
Available online 24.04.2021 with doi: 10.5455/medscience.2020.10.217

Abstract

In this study, a new 2.5-substituted benzoxazole derivative compound was synthesized in three steps, its antimicrobial activities were determined by the microdilution method on Staphylococcus aureus ATCC 29213, *Enterococcus faecalis ATCC 29212, Escherichia coli* ATCC 25922, *Pseudomonas aeruginosa* ATCC 27853, *Candida albicans* ATCC 10231 and their isolates, and also *in silico* studies were performed. The structure of the compound was illuminated by 1H-NMR and 13C-NMR spectroscopy and HRMS, and the resulting analysis results proved our structure. When the antimicrobial activity results were examined, although the reference drugs generally showed better antimicrobial activity, it was observed that the synthesized compound showed very promising activity against Candida albicans isolate with MIC: 16 ug/mL. Molecular docking studies were conducted to understand the mechanism of the compound's good antimicrobial effect against *Candida albicans* isolate (PDB: 5TZ1). Estimated ADME profiles were determined. In addition, quantum chemical calculations were made with the DFT/B3LYP method in the 6-311G (d,p) basic set, the structural properties, geometry, electronic and thermodynamic properties of the molecule were determined and the results were displayed.

Keywords: Antimicrobial activity, benzoxazole DFT, molecular docking

Introduction

Infectious diseases represent an increasing global public health problem. There are many types of bacterial infectious diseases and the participation of fungi in the etiology of infectious diseases has also increased significantly. With the importance of antimicrobial drugs in treatment, resistance to these drugs is also a serious danger. One of the two important factors leading to the development of resistance is the widespread use of antimicrobials for other than appropriate indications, and the other is the use of under therapeutic dose and inadequate time. Such uses increase microorganism colonization and result in the selection of resistant mutants [1]. Resistance to antimicrobials may vary according to time and geography, the body area where the bacteria is isolated, infection in the community or hospital, patient characteristics (age, immune system, underlying disease, living in the crowded environment), last antibiotic treatment, length of hospital stay, and sensitivity tests applied [2]. For all these reasons, there is a need to discover new effective antimicrobial drugs.

Benzoxazole ring is one of the important heterocyclic compounds in medicinal chemistry. Pharmacological action studies for benzoxazole ring include antibacterial/antifungal [3], antimycobacterial [4], antiviral [5], antiparkinsonian [5], antioxidant [6], antihypertensive [7], antitumoral [8], anti-inflammatory [9], herbicidal [10], antialzheimer's activity studies [11]. When the open chemical structure of this ring system is examined, it is seen that it is an analog of adenine and guanine bases in the structure of nucleic acids and it is thought that it can achieve its antimicrobial effect by inhibition of nucleic acid synthesis or DNA gyrase enzyme inhibition [12]. Although there are many studies in the literature on the synthesis and pharmacological activities of 2,5-disubstituted benzoxazoles, studies on quantum chemical calculations of these compounds are limited. This study was carried out in two parts. In the first part, the new 2.5-disubstituted benzoxazole compound was synthesized, its structures were illuminated by ^{1}H-NMR and ^{13}C-NMR spectroscopy and HRMS, and its antimicrobial activities were investigated. In the second part; molecular docking studies were carried out, quantum chemical calculations were made with the DFT/B3LYP method in the 6-311G (d,p) basic set, and the structural properties, geometry, electronic and thermodynamic properties of the molecule were determined.

*Corresponding Author: Meryem Erol Erciyes University, Faculty of Pharmacy, Department of Pharmaceutical Chemistry, Kayseri, Turkey
E-mail: eczacimeryem@gmail.com

Material and Methods

Chemistry

Chemicals and solvents were purchased from Sigma-Aldrich, Across Organics, Merck, Riedel de Haen, and Fluka and used without further purification. Thin Layer Chromatography (TLC) was used to monitor the progress of the reaction during the synthesis studies and to determine the purity levels of the product obtained. [M+1] peaks of the synthesized compounds were determined using an Agilent 6224 Line-Mass TOF LC/MS system (Agilent Technologies, CA, USA). ^{1}H and ^{13}C NMR spectra were taken in Varian Mercury-400 Agilent FT-NMR spectrometer, using dimethylsulfoxide-d_6 (DMSO-d_6). Melting point determinations were made by the capillary method using an Electrothermal 9100 device and given uncorrected.

General procedure for the preparation of 2-(p-fluorophenyl)-5-(2-(4-phenylpiperidine-1-yl)acetamido)benzoxazole

The target product M1 was obtained by the general procedure method given in Figure 1. In the first step, 2,4-diaminophenol dihydrochloride was reacted with p-fluoro benzoic acid for 3 h at 160-190ºC in the presence of polyphosphoric acid (PPA). At the end of the period, it was poured into ice and made basic with 10% NaOH. Filtered, crystallized from ethanol-water. The ring was closed with this reaction and the benzoxazole compound was obtained. For the amidification in step 2, it was treated with chloroacetyl chloride at room temperature overnight. At the end of the period, it was filtered, crystallized from ethanol-water. In the last step, this amide derivative was reacted with 4-phenyl piperidine in the presence of dimethylformamide (DMF) and triethylamine (TEA) for 1 day at room temperature. Water was poured over it, precipitated, then crystallized from ethanol-water and the target product was obtained [13-16].

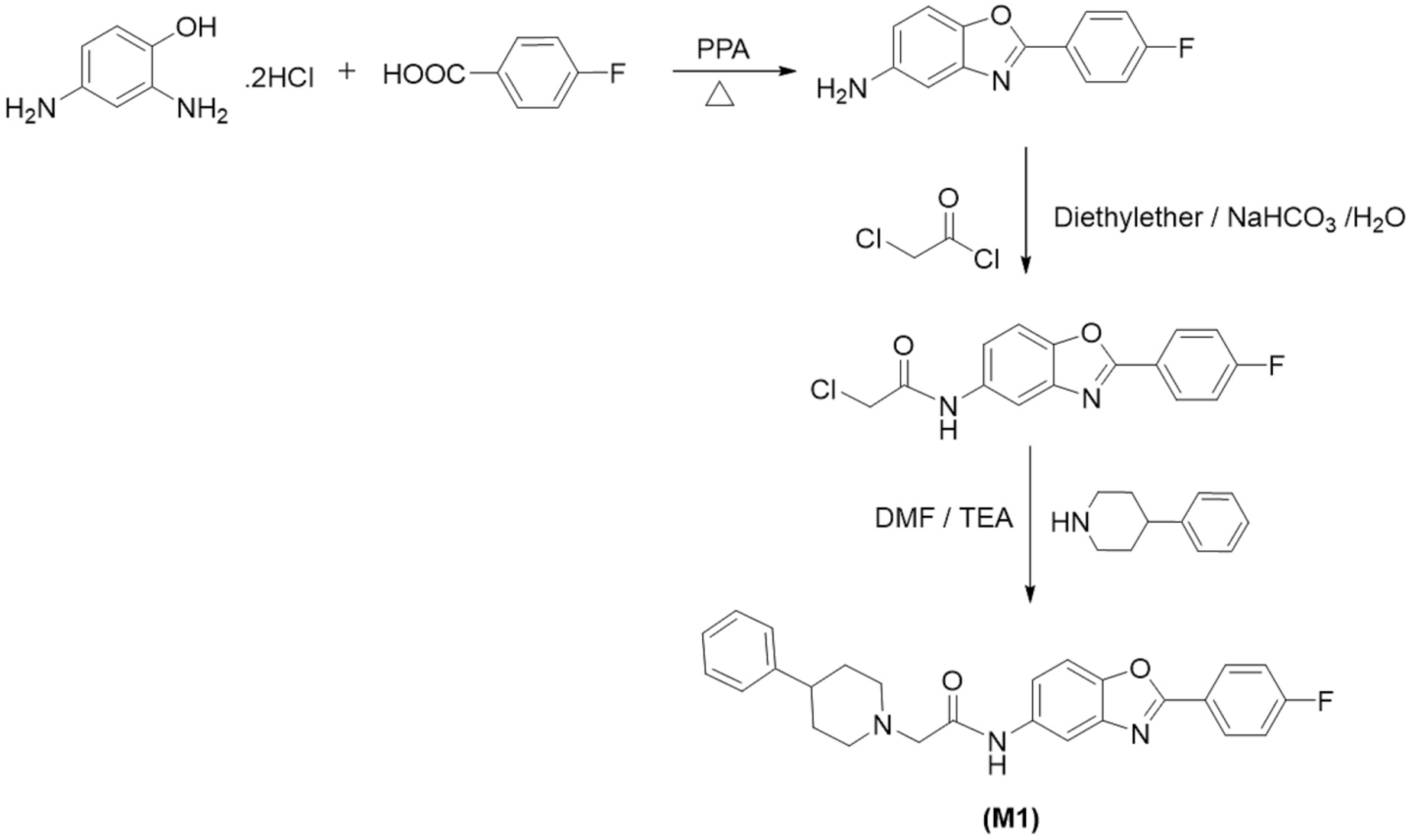

Figure 1. General procedure for the preparation of M1

Antimicrobial evaluation

In this assay, the sensitivity of some microorganisms to compound synthesized in the first stage of our experiment was examined according to the Clinical Laboratory Standards Institute (CLSI) M100-S28 protocol [17] for bacteria and CLSI M27-A3 protocol for fungi [18]. The potential antibacterial activity of these compounds was tested against Staphylococcus aureus ATCC 29213, Enterococcus faecalis ATCC 29212, Escherichia coli ATCC 25922, Pseudomonas aeruginosa ATCC 27853, and isolates of these bacteria in Mueller Hinton Broth (MHB) medium. And also, the potential antifungal activity of these compounds was tested against Candida albicans ATCC 10231 and its isolate in RPMI-1640 medium. First, the stock solutions of the compounds were prepared in DMSO at a concentration of 12.8 mg/ml. The serial dilutions of M1 (256 µg/mL, 128 µg/mL, 64 µg/mL, 32 µg/mL, 16 µg/mL, 8 µg/mL, 4 µg/mL, 2 µg/mL) were prepared in 96-well microplates, after placing medium in each microplate-well. The suspension of microorganisms was prepared using 0.5 McFarland standard and inoculated to each well to be 10^5 CFU/mL at final density. Bacteria were incubated for 24 h at 37ºC and fungus for 48 h at 35ºC. The activity of reference antibiotics prepared in serial dilution was tested on the same microorganisms. Besides, growth control of microorganisms and sterilization control of the medium was also tested in each microplate. All assays were carried out in triplicate.

Molecular docking

Crystal structure of sterol 14-alpha demethylase (CYP51) from Candida albicans in complex with the tetrazole-based antifungal drug candidate VT1161 (PDB ID: 5TZ1 at 2.00 Å resolution) were imported from protein data bank (https://www.rcsb.org/). The 'A' chain in the 5TZ1 structure was selected. The active site was created coordinates x: 70.610, y: 66.284, z: 4.177, and 20x20x20 Å. Protein was prepared in pdbqt file format using AutoDockTools 1.5.6 program [19]. Ligands were drawn with the Chem3D 19.0 program, minimized, saved in pdb format. And converted to pdbqt file format with AutoDockTools 1.5.6 program. The molecular docking process was carried out with the latest AutoDock Vina program [20]. The results were displayed in 2D and 3D with the PyMOL [21] and Discovery Studio 2020 Client program [22].

Computational details

Quantum chemical calculations of all compounds were done using the Gaussian 09 package program [23] and Density Functional Theory (DFT)/B3LYP/6-311G (d,p) method. The molecular geometry characteristics (optimized molecular structure, bond lengths, bond angles), electrochemical properties (HOMO-LUMO, electronegativity, chemical hardness, electrophilic index, and softness), molecular electrostatic potential (MEP) of the compound were determined by theoretical calculations. GaussView 6 program [24] was used for molecule visualization. To evaluate ADME profiles of compounds; were calculated using the Molinspiration software program [25]. Drug-likeness scores were calculated using the Molsoft program [26].

Results

Chemistry

^{1}H and ^{13}C NMR, HRMS data of compound M1 were as follows: Yield 62%, Mp: 172-175^{0}C.^{1}H-NMR δ ppm (400 MHz, DMSO-d^{6}): 9.81 (s, H, amide -NH), 8.22–8.16 (m, 3H, H-2', 6', 4), 7.60 (dd, J = 20.9, 8.3 Hz, 4H, H-3', 5', 6, 7), 7.31 (d, J = 6.5 Hz, 4H, H-2'',3'',5'',6''), 7.22 (t, J = 6.8 Hz, 1H, H-4''), 3.05 (s, 2H, -NH-CO-CH^{2}), 3.02 (d, J = 11.1 Hz, 2H, piperidine -CH^{2}), 2.21 (t, J = 11.2 Hz, 2H, piperidine -CH2), 1.75 – 1.61 (m, 5H, piperidine -CH^{2} and -CH) (Figure 2). ^{13}C-NMR δ ppm (100 MHz, DMSO-d^{6}): 168.45, 164.51, 147.92, 146.70, 143.31, 136.58, 132.41, 128.85, 128.84, 127.65, 127.21, 126.48, 124.32, 115.85, 110.72, 110.51, 60.51, 52.68, 42.74, 33.15. HRMS (m/z): [M+H]+ calcd for C^{26}H^{24}FN^{3}O^{2}: 430.18526; found: 430.19385. The analysis results confirmed the structure of the compound.

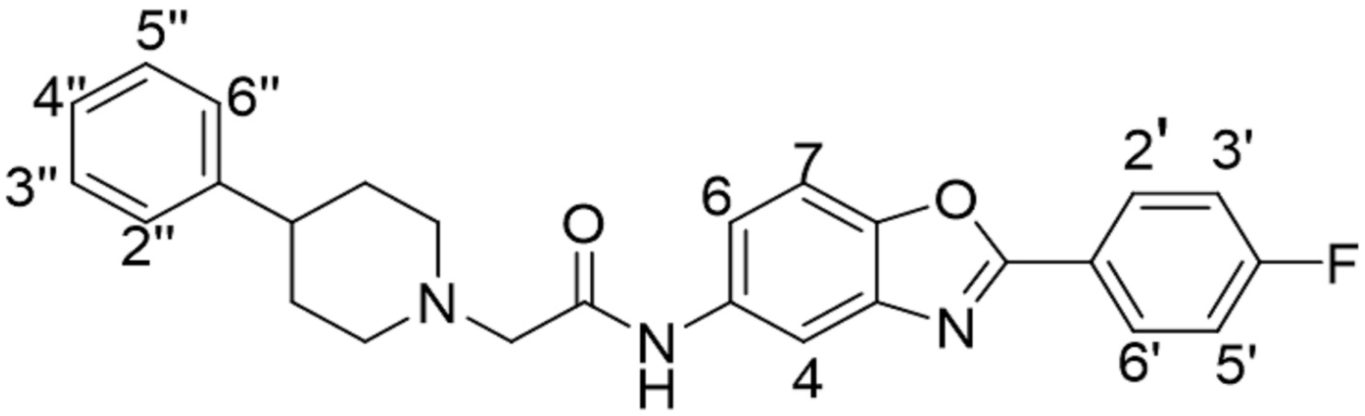

Figure 2. Number locations in detailed ^{1}H-NMR analysis of the M1

Antimicrobial evaluation

The data on the antimicrobial activity of the M1 and the reference drugs as MIC (µg/mL) values were given in Table 1. According to the results, although the antimicrobial activity of the M1 was lower compared to some known reference drugs, it exhibited broad antibacterial activity with MIC values in the range of 32–256 µg/mL. While it showed activity against C. albicans with 64 µg/mL, it showed very promising activity against C. albicans isolate with 16 µg/mL. These promising results showed that drug-resistant C. albicans could be the leading compounds to find new antifungal candidates.

Molecular docking study

The mechanism of resistance in C. albicans may be a change in lanosterol demethylase (Erg11p) and ergosterol biosynthesis [27, 28]. Therefore, we focused on the sterol 14α-demethylase (CYP51) protein (PDB: 5TZ1), as M1 showed very high activity against the C. albicans isolate. M1 and VT1 showed binding energy of -12.5 and -12.1 kcal/mol, respectively, and 2D protein-ligand interactions were showed in Figure 3. M1 formed pi-sigma bond with HEM A601, pi-alkyl bond with PRO A230, LEU A376, ILE A131, TYR A132, and pi-pi T-shaped bond with HIS A377. Both ligands showed similar hydrophobic interactions.

*(R)-2-(2,4-Difluorophenyl)-1,1-difluoro-3-(1H-tetrazol-1-yl)-1-(5-(4-(2,2,2-trifluoroethoxy)phenyl)pyridin-2-yl)propan-2-ol

In silico ADME estimation

According to Lipinski's five rules, the molecular weight should be ≤500, the molecule logP≤5, the number of hydrogen bond receptors ≤10, and the number of hydrogen bond donors should be ≤5 [29]. Accordingly, M1 complies with all but logP and conforms to the Lipinski rule. The percent absorption (% ABS) was calculated with the formula % ABS = 109- (0.345 x TPSA) [30] and showed a good absorption profile with 88.86%. It also has a good drug-likeness score of 1.32. The estimated ADME parameters calculated were given in Table 2.

Table 1. In vitro antimicrobial activity of M1 in comparison with the reference drugs (MIC values in µg/mL).

	Gram-positive bacteria				Gram-negative bacteria				Fungi	
Compound	S.a	S. a.*	E.f.	E.f.*	E.c.	E.c.*	P.a.	P.a.*	C.a.	C.a*
M1	128	128	64	128	128	128	64	64	64	16
Ampicillin	2	>16	2	>16	8	>16	-	-	-	-
Vancomycin	2	2	1	8	-	-	-	-	-	-
Gentamycin	0.25	>16	-	-	0,5	>8	0,5	>8	-	-
Ciprofloxacin	0.5	>16	2	>4	0.0156	>2	0.125	>2	-	-
Cefotaxime	1	>16	-	-	0.125	>8	8	-	-	-
Fluconazole	-	-	-	-	-	-	-	-	0.125	>4
Amphotericin B	-	-	-	-	-	-	-	-	0.5	0.5

S.a.: Staphylococcus aureus ATCC 29213; S.a.: S. aureus isolate; E.f: Enterococcus faecalis ATCC 29212; E.f *: E. faecalis isolate (Vancomycin resistant -VREF); E.c.: E. coli ATCC 25922; E.c.*: E. coli isolate (contains broad spectrum β-lactamase enzyme -GSBL-); P.a.: Pseudomonas aeruginosa ATCC 27853; P.a.*: P. aeruginosa isolate (gentamicin resistant); (MRSA); C.a: Candida albicans ATCC 10231; C. a.*: Candida albicans isolate*

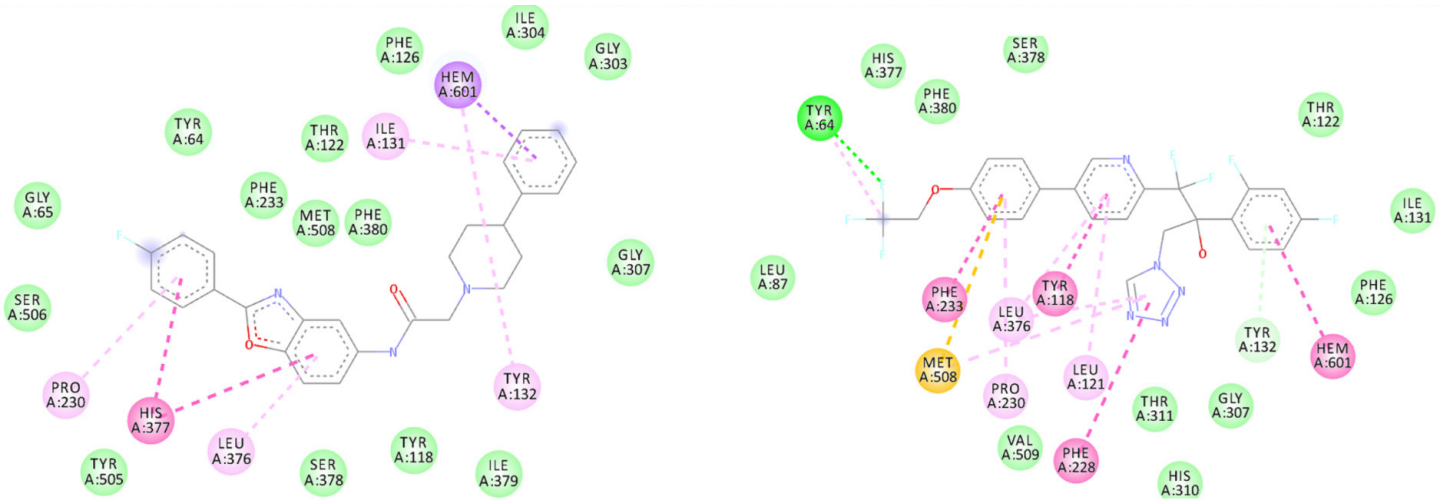

Figure 3. 2D protein-ligand interactions of M1 (left) and VT1*(right)

Table 2. Calculated ADME parameters

LogP (≤5)	5.83	nOHNH (≤5)	1
TPSA (-)	58.37	nviolations (≥1)	1
% ABS (-)	88.86	nrotb (-)	5
MW (≤500)	429.50	Volume (-)	387.36
nON (≤10)	5	Drug-likeness score	1.32

MW: Molecular weight. TPSA: Topological polar surface area. %ABS: Percentage absorption. nrotb: Number of rotatable bonds. nON: Number of hydrogen acceptors. nOHNH: Number of hydrogen donors. LogP: Log octanol/water partition coefficient

Frontier molecular orbital analysis

The frontier molecular orbitals (FMO), called the highest occupied molecular orbitals (HOMO) and the lowest unoccupied molecular orbitals (LUMO), play an important role in quantum chemistry and electronic, electrical, and optical properties. Since most chemical reactions are by electron exchange, the boundary orbitals determine the chemical behavior of the molecule. LUMO is the lowest energy orbital capable of accepting electrons and hence acts as an electron acceptor, characterizing the susceptibility of the molecule to attacks by nucleophiles. HOMO is the highest energy orbital containing electrons and therefore acts as an electron donor. The energy difference between the HOMO and LUMO energies, called the energy gap, helps to characterize the chemical reactivity and kinetic stability of the molecule [31, 32]. HOMO and LUMO values of M1 were -0.20567 a.u. (-5,59657 eV) and 0.16044 a.u. (-1,23077 eV). Also, the energy difference (optical band gap energy) between HOMO and LUMO orbitals for this molecule is 0.42589 a.u. (4,3657 eV). At the same time, the electrochemical properties (ionization potential (IP), electron affinity (EA), electronegativity (X), chemical hardness (η), chemical softness (S), chemical potential (μ) and electrophilic index (ω)) were calculated using HOMO and LUMO energies [33], and the results obtained were given in Table 3. HOMO of M1 is delocalized on the whole molecule except piperidine and phenyl ring, and its LUMO is delocalized on the whole molecule except the amide group, piperidine, and phenyl ring (Figure 4).

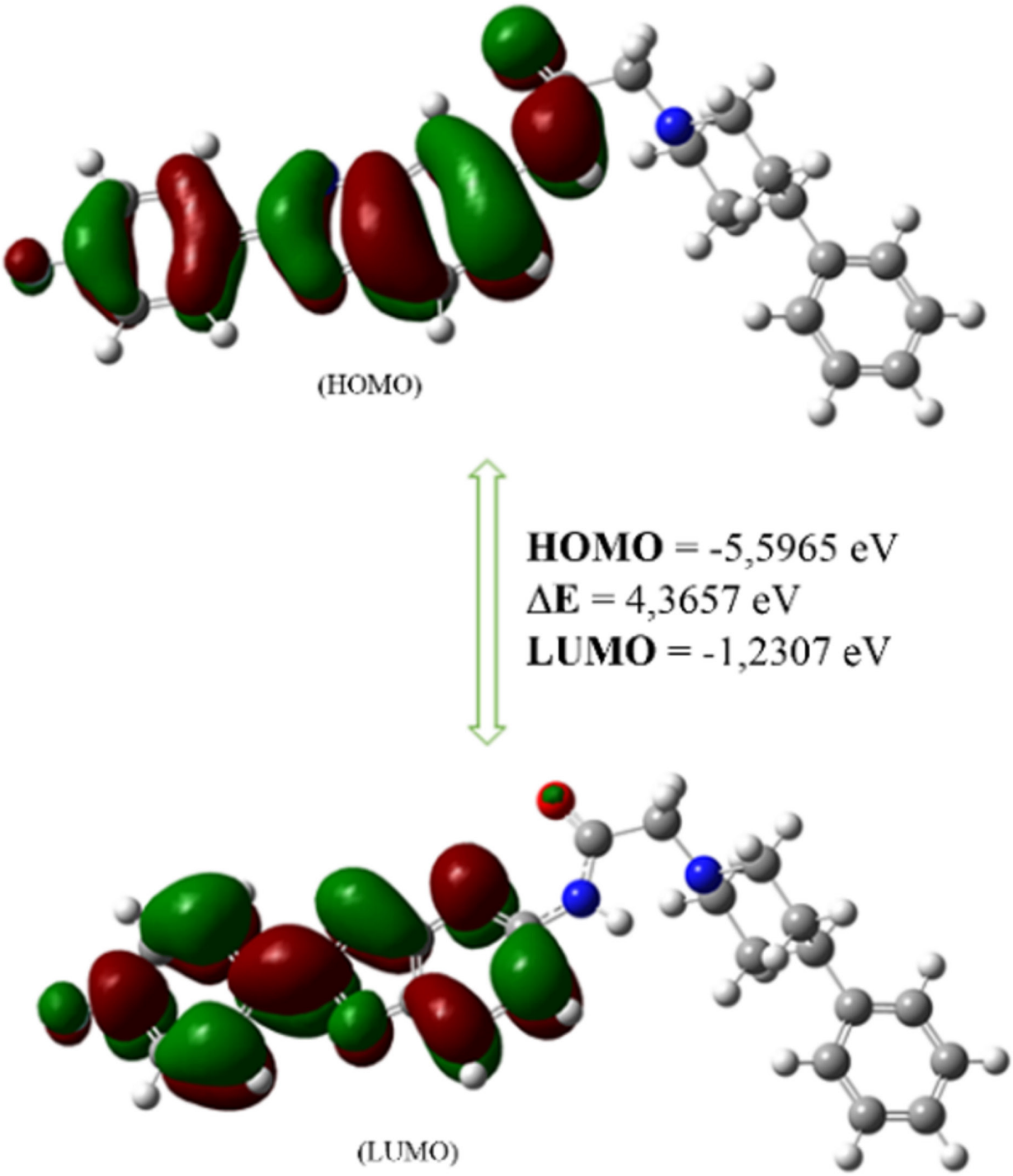

Figure 4. HOMO and LUMO plots of M1

Table 3. Calculated quantum chemistry descriptors of M1

Energy (Hartree)	-1420.1517
Dipol moment (Debye)	5.5074
HOMO	-5.5965
LUMO	-1,2307
ΔE= LUMO-HOMO	4.3657
IP = (-HOMO)	5.5965
EA = (-LUMO)	1.307
ṅ= (*I*P−EA/)2	2.1828
μ = −(IP+EA)/2	-3.4136
S = (1/2ṅ)	0.2290
X= (*I*P+E*A*)/ 2	3.4136
ω = (μ2 /2η)	1.3345

Molecular electrostatic potential

Molecular electrostatic potential (MEP) is an important theoretical property showing the charge distributions of a molecule. Therefore, the MEP map of the M1 has been studied in detail to determine the electrophilic interaction, nucleophilic reactions, hydrogen bond interactions, and especially how it will interact with other molecules. In addition, MEP characterization is very important to understand the size and shape of the molecule. The red regions in the map indicate electrophilic activity, the blue regions indicate nucleophilic activity, and the green/yellow regions indicate neutral sites. In other words, the red regions denote regions with high electron density and the blue regions represent regions with low electron density [34, 35]. Intermediate electrostatic potentials are between red and blue potentials according to the following order: red<orange<yellow<green<blue [36]. The MEP map of the compound was shown in Figure 2. When the MEP map of the synthesized compound is examined, it is seen that the molecule has areas rich in both positive and negative regions. In the MEP map of M1 (Figure 5); the red regions are mainly concentrated on the oxygen and nitrogen atoms. When the MEP map of the synthesized compound is examined, it is seen that the molecule has areas rich in both positive and negative regions. In the MEP map t has been observed that the red regions are mainly concentrated on oxygen and nitrogen atoms, while the green regions are concentrated around carbon and hydrogen atoms.

Geometrical parameters

In the theoretical calculation of molecular energy and other properties, the geometry of the molecule is very important. The coordinates of the electrons in the molecule depend on the arrangement of the atoms, and the arrangement of the atoms on the molecular geometry. Even the smallest changes in molecular geometry affect the energy of the molecule. Geometric optimization is the release of the geometry of the molecule originally defined to the program, allowing the program to bring the molecule to its most stable geometry. The most stable states of molecules also correspond to atomic arrays in which their energy is minimum. Geometric optimization is also known as gradient optimization or force method. All calculations are made when the molecular structure is in a certain geometry, and any change in the molecular structure causes the energy and many other properties of the molecule to change [37]. The numbered optimized geometrical structure of M1 was given in Figure 6. The some important calculated bond angles are N(11)-C(12)-O(14); 124.7326º, N(7)-C(8)-O(9); 111.6332º, C(22)-C(23)-F(26); 120.5495º; N(11)-C(12)-H(36); 116.3538º, C(5)-O(9)-C(8); 106.8366º. The some calculated bond lengths are C(5)-O(9); 1.2256 Å, C(4)-N(7); 1.2617 Å, N(11)-C(12); 1.3631 Å, C(23)-F(26); 1.3232 Å, N(7)-C(8); 1.2723 Å., the bond lengths (Å), bond angles (º), and dihedral angles were presented in Table 4 and Table 5.

Discussion

In this study, synthesis of 2,5-disubstituted benzoxazole compound (M1), and characterization by ^{1}H-NMR, ^{13}C-NMR spectroscopy, and HRMS were performed. Antimicrobial activity was determined against various strains by microdilution method. M1 showed weak antibacterial activity against reference drugs against the structures examined, while activity very close to fluconazole against C. albicans. Molecular docking studies were performed on the '5TZ1' structure and M1 and VT1 showed similar binding interactions. The ADME profiles comply with Lipinski and other restrictive rules. Quantum chemical calculations were calculated with the DFT/B3LYP method and the 6-311G (d,p) basis set. The geometric parameters (bond lengths, bond angles, and dihedral angles) of the optimized structure were determined theoretically. In addition, electronic parameters such as electron affinity, ionization potential, nucleophilic properties, and molecular hardness-softness were calculated using HOMO-LUMO orbital energies. In addition, it was observed that the MEP map of the molecule has areas rich in both positive and negative regions, electron-rich regions (red region) are concentrated around oxygen and nitrogen atoms, and neutral regions are concentrated around carbon and hydrogen atoms (green region). It showed an overall good theoretic ADME profile. The theoretical study is very important and necessary in order to identify the compounds with antimicrobial properties and to reveal their structural properties in future drug development studies. When all the results are evaluated together, this study will make an important contribution to the studies carried out to develop safe and potent drugs, especially since pathogens develop resistance to the drugs used in current treatment methods and M1 may be a promising antifungal agent.

Table 4. Calculated bond lengths (Å) and bond angles (º) of M1

Bond Length	B3LYP	Bond length	B3LYP	Bond Angle	B3LYP	Bond Angle	B3LYP	Bond Angle	B3LYP
C1,C2	1.3512	C19,C20	1.5376	C2,C1,C6	122.4777	N15,C13,H37	111.5289	H46,C20,H47	106.9712
C1,C6	1.3447	C19,H44	1.1154	C2,C1,H33	119.8671	N15,C13,H38	110.5917	C10,C21,C22	121.3534
C1,H33	1.1043	C19,H45	1.1163	C6,C1,3H3	117.6552	H37,C13,H38	107.4493	C10,C21,H48	121.3156
C2,C3	1.3478	C20,H46	1.1171	C1,C2,C3	118.9786	C13,N15,C16	111.3019	C22,C21,H48	117.3309
C2,N11	1.3492	C20,H47	1.1161	C1,C2,N11	114.964	C13,N15,C20	111.0121	C21,C22,C23	120.4431
C3,C4	1.3381	C21,C22	1.3426	C3,C2,N11	126.0574	C16,N15,C20	111.0333	C21,C22,H49	119.9678
C3,H34	1.0976	C21,H48	1.1031	C2,C3,C4	118.4073	N15,C16,C17	111.5984	C23,C22,H49	119.589
C4,C5	1.3326	C22,C23	1.341	C2,C3,H34	123.8314	N15,C16,H39	110.5507	C22,C23,C24	118.904
C4,N7	1.2617	C22,H49	1.1029	C4,C3,H34	117.7613	N15,C16,H40	110.6205	C22,C23,F26	120.5495
C5,C6	1.337	C23,C24	1.341	C3,C4,C5	121.9132	C17,C16,H39	107.8788	C24,C23,F26	120.5465
C5,O9	1.2256	C23,F26	1.3232	C3,C4,N7	132.8445	C17,C16,H40	109.2823	C23,C24,C25	120.4275
C6,H35	1.1015	C24,C25	1.3424	C5,C4,N7	105.2423	H39,C16,H40	106.7515	C23,C24,H50	119.5973
N7,C8	1.2723	C24,H50	1.1029	C4,C5,C6	120.9047	C16,C17,C18	110.4899	C25,C24,H50	119.9751
C8,O9	1.2379	C25,H51	1.1033	C4,C5,O9	109.6146	C16,C17,H41	108.5114	C10,C25,C24	121.3757
C8,C10	1.3487	C27,C28	1.3463	C6,C5,O9	129.4802	C16,C17,H42	110.1044	C10,C25,H51	121.2492
C10,C21	1.3477	C27,C32	1.3461	C1,C6,C5	117.3179	C18,C17,H41	110.5436	C24,C25,H51	117.375
C10,C25	1.3479	C28,C29	1.3422	C1,C6,H35	121.6874	C18,C17,H42	109.8674	C18,C27,C28	120.7746
N11,C12	1.3631	28,52	1.1026	C5,C6,H35	120.9946	41,17,42	107.2606	C18,C27,C32	121.3443
N11,H36	1.0106	C29,C30	1.3411	C4,N7,C8	106.6733	C17,C18,C19	108.9879	C28,C27,H32	117.8811
C12,C13	1.523	C29,H53	1.103	N7,C8,O9	111.6332	C17,C18,C27	112.3	C27,C28,C29	121.274
C12,O14	1.2042	C30,C31)	1.341	N7,C8,C10	124.9809	C17,C18,H43	107.0214	C27,C28,H52	120.2058
C13,N15	1.459	C30,H54	1.1027	O9,C8,C10	123.3846	C19,C18,C27	112.4177	C29,C28,H52	118.5203
C13,H37	1.1146	C31,C32	1.3422	C5,O9,C8	106.8366	C19,C18,H43	106.9791	C28,C29,C30	120.048
C13,H38	1.1163	C31,H55	1.1031	C8,C10,C21	121.44	C27,C18,H43	108.8557	C28,C29,H53	120.067
N15,C16	1.4584	C32,H56	1.1019	C8,C10,C25	121.0638	C18,C19,C20	110.6426	C30,C29,H53	119.885
N15,C20	1.4573			C21,C10,C25	117.4962	C18,C19,H44	110.4233	C29,C30,C31	119.4637
C16,C17	1.5371			C2,N11,C12	133.3708	C18,C19,H45	109.8771	C29,C30,H54	120.2728
C16,H39	1.1162			C2,N11,H36	110.2659	C20,C19,H44	108.5012	C31,C30,H54	120.2635
C16,H40	1.116			C12,N11,H36	116.3538	C20,C19,H45	110.0834	C30,C31,C32	120.0551
C17,C18	1.5358			N11,C12,C13	113.3468	H44,C19,H45	107.2434	C30,C31,H55	119.8898
C17,H41	1.1154			N11,C12,O14	124.7326	N15,C20,C19	111.681	C32,C31,H55	120.0551
C17,H42	1.1163			C13,C12,O14	113.2578	N15,C20,H46	110.1078	C27,C32,C31	121.2782
C18,C19	1.5358			C12,C13,N15	110.838	N15,C20,H47	110.5284	C27,C32,H56	120.3037
C18,C27	1.52			C12,C13,H37	110.7978	C19,C20,H46	107.9343	C31,C32,H56	118.4181
C18,H43	1.1187			C12,C13,H38	105.4095	C19,C20,H47	109.4717		

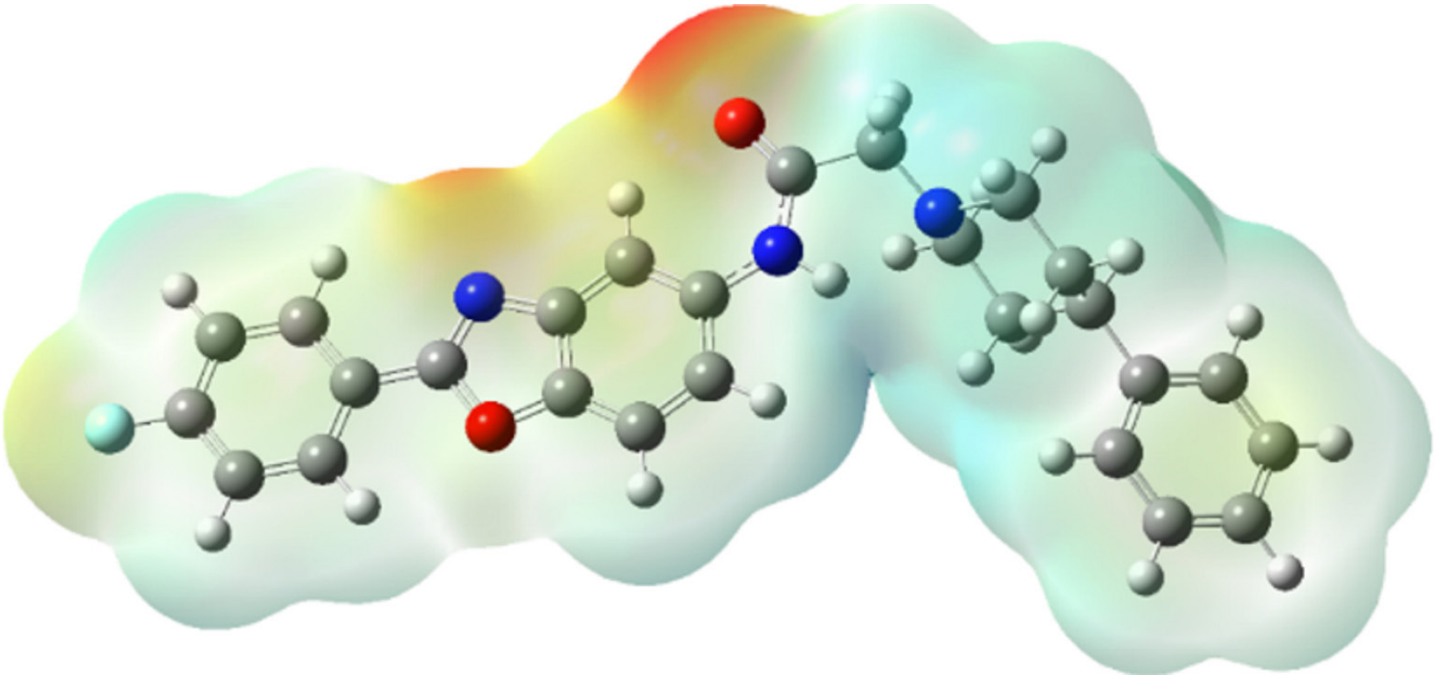

Figure 5. MEP map of M1

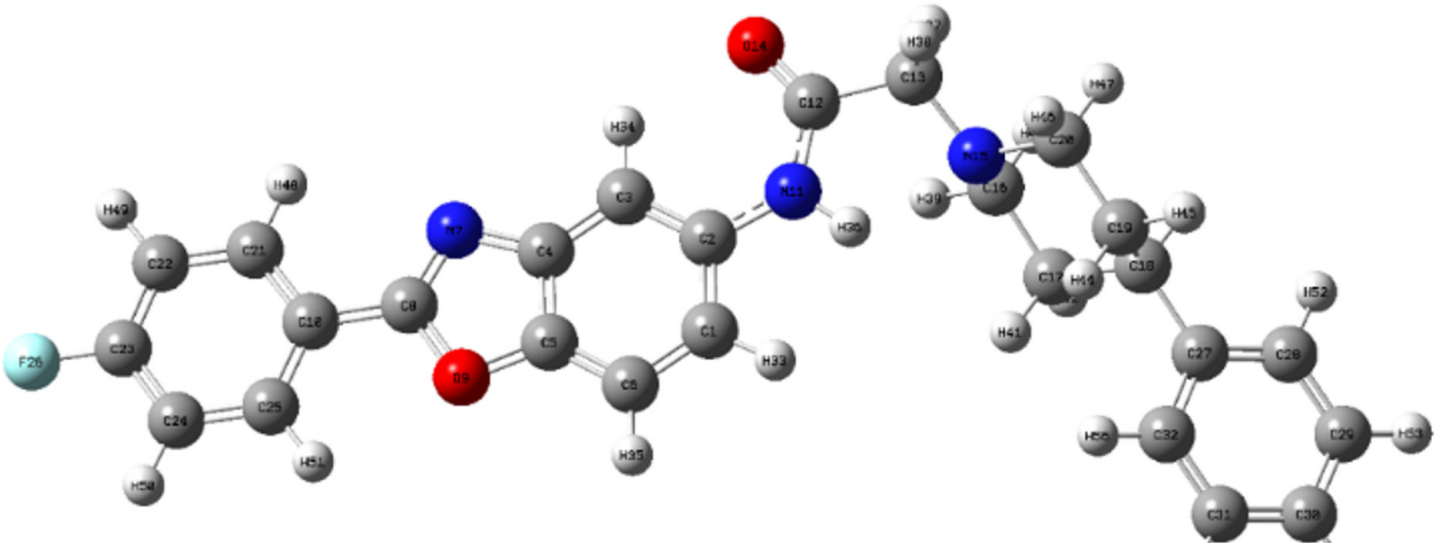

Figure 6. Optimized molecular structure of M1

Table 5. Calculated selected dihedral angles (º) of M1

Dihedral angles	B3LYP	Dihedral angles	B3LYP
C6,C1,C2,C3	0.0367	C13,N15,C20,C19	176.9278
H33,C1,C2,C3	179.9996	N15,C16,C17,H42	-178.908
C2,C1,C6,C5	0.1666	H40,C16,C17,H41	-173.3533
C1,C2,C3,C4	-0.1267	C16,C17,C18,C27	179.6171
N11,C2,C3,H34	-0.1604	C17,C18,C19,H45	-175.9261
C3,C2,N11,C1	-0.9092	C10,C21,C22,C23	0.0343
C2,C3,C4,N7	-179.9972	C18,C27,C28,C29	-179.9524
C5,C4,N7,C8	0.0367	C8,C10,C25,H51	0.106
C4,C5,O9,C8	-0.006	H36,N11,C12,C13	-0.7312
C10,C8,N9,C5	-179.5746	H38,C13,N15,C16	-174.8315
C13,N15,C16,C17	-176.8268	C20,N15,C16,H39	179.0295

Conflict of interests
The authors declare that they have no competing interests.

Financial Disclosure
All authors declare no financial support.

References

1. Alanis AJ. Resistance to antibiotics: are we in the post-antibiotic era? Arch Med Res. 2005;36:697-705.
2. Blair JM, Webber MA, Baylay AJ, et al. Molecular mechanisms of antibiotic resistance. Nat Rev Microbiol. 2015;13:42-51.
3. Erol M, Celik I, Temiz-Arpaci O, et al. Design, synthesis, molecular docking, density functional theory and antimicrobial studies of some novel benzoxazole derivatives as structural bioisosteres of nucleotides. J Biomol Struct Dyn. 2020;1-12.
4. Arisoy M, Temiz-Arpaci O, Kaynak-Onurdağ F, et al. Antimycobacterial properties of some 2, 5-disubstituted-benzoxazole derivatives. J Fac Pharm Ankara. 2010;39:155-62.
5. Rida SM, Ashour FA, El-Hawash SA, et al. Synthesis of some novel benzoxazole derivatives as anticancer, anti-HIV-1 and antimicrobial agents. Eur J Med Chem. 2005;40:949-59.
6. Abdelgawad MA, Bakr RB, Ahmad W, et al. New pyrimidine-benzoxazole/benzimidazole hybrids: Synthesis, antioxidant, cytotoxic activity, in vitro cyclooxygenase and phospholipase A2-V inhibition. Bioorg Chem. 2019;92:1-6.
7. Wu Z, Bao X-L, Zhu W-B, et al. Design, synthesis, and biological evaluation of 6-benzoxazole benzimidazole derivatives with antihypertension activities. ACS Med Chem Lett. 2018;10:40-3.
8. Yuan X, Yang Q, Liu T, et al. Design, synthesis and in vitro evaluation of 6-amide-2-aryl benzoxazole/benzimidazole derivatives against tumor cells by inhibiting VEGFR-2 kinase. Eur J Med Chem. 2019;179:147-65.
9. Angajala G, Subashini R. Synthesis, molecular modeling, and pharmacological evaluation of new 2-substituted benzoxazole derivatives as potent anti-inflammatory agents. Struct Chem. 2020;31:263-73.
10. Sangi DP, Meira YG, Moreira NM, et al. Benzoxazoles as novel herbicidal agents. Pest Manag Sci. 2019;75:262-9.
11. Celik I, Erol M, Temiz Arpaci O, et al. Evaluation of activity of some 2, 5-disubstituted benzoxazole derivatives against acetylcholinesterase, butyrylcholinesterase and tyrosinase: ADME prediction, DFT and comparative molecular docking studies. Polycycl Aromat Compd. 2020;1-12
12. Oehlers L, Mazzitelli CL, Brodbelt JS, et al. Evaluation of complexes of DNA duplexes and novel benzoxazoles or benzimidazoles by electrospray ionization mass spectrometry. J Am Soc Mass Spectrom. 2004;15:1593-603.
13. Erol M, Celik I, Uzunhisarcikli E, et al. Synthesis, molecular docking, and DFT studies of some new 2,5-disubstituted benzoxazoles as potential antimicrobial and cytotoxic agents. Polycycl Aromat Compd. 2020;1-18.
14. Arisoy M, Temiz-Arpaci O, Kaynak-Onurdag F, et al. Synthesis of some piperazinobenzoxazole derivatives and their antimicrobial properties. Indian J Chem. 2016;55:240-7.
15. Taşcı M, Temiz-Arpaci O, Kaynak-Onurdag F, et al. Synthesis and antimicrobial evaluation of novel 5-substituted-2-(p-tert-butylphenyl) benzoxazoles. Indian J Chem. 2018;57:385-9.
16. Arisoy M, Temiz-Arpaci O, Kaynak-Onurdag F, et al. Synthesis and antimicrobial activity of novel benzoxazoles. Z Naturforsch C J Biosci. 2012;67:466-72.
17. CaLSI C. Performance Standards for Antimicrobial Susceptibility Testing: Approved Twenty-: Document M100-S28. Wayne, PA, USA: CLSI. 2018.
18. dition AS-S. CLSI document H3-A6. Wayne (PA): CLSI. 2007.
19. Huey R, Morris GM. Using AutoDock 4 with Auto Docktools: a tutorial. The Scripps Research Institute, USA. 2008;54-6.
20. Trott O, Olson AJ. Auto Dock Vina: improving the speed and accuracy of docking with a new scoring function, efficient optimization, and multithreading. J Comput Chem. 2010;31:455-61.
21. Lill MA, Danielson ML. Computer-aided drug design platform using PyMOL. Journal of computer-aided molecular design. 2011;25:13-9.
22. Biovia DS. Discovery studio visualizer. San Diego, CA, USA. 2017;936.
23. Frisch M, Trucks G, Schlegel H, et al. Gaussian 09 (Revision A. 02) [Computer software]. Gaussian Inc, Wallingford CT. 2009.
24. GaussView V. 6, Roy Dennington, Todd A. Keith, and John M Millam, Semichem Inc, Shawnee Mission, KS. 2016.
25. Cheminformatics M. Calculation of molecular properties and bioactivity score. Computer software] Retrieved from http://www molinspiration com/cgi-bin/properties.
26. Molsoft L. ICM software manual. Version; 2004.
27. Sanglard D, Odds FC. Resistance of Candida species to antifungal agents: molecular mechanisms and clinical consequences. The Lancet infectious diseases. 2002;2:73-85.
28. Morschhäuser J. The genetic basis of fluconazole resistance development in Candida albicans. Biochimica et Biophysica Acta (BBA)-Molecular Basis of Disease. 2002;1587:240-8.
29. Lipinski CA. Lead-and drug-like compounds: the rule-of-five revolution. Drug Discov Today Technol. 2004;1:337-41.
30. Kilic-Kurt Z, Bakar-Ates F, Bahat M. N, N′-diaryl urea derivatives: Molecular docking, molecular properties prediction and anticancer evaluation. J Mol Struct. 2019;1193:239-46.
31. Beegum S, Panicker CY, Armaković S, et al. Spectroscopic, antimicrobial and computational study of novel benzoxazole derivative. J Mol Struct. 2019;1176:881-94.
32. Algul O, Ersan RH, Alagoz MA, et al. An efficient synthesis of novel di-heterocyclic benzazole derivatives and evaluation of their antiproliferative activities. J Biomol Struct Dyn. 2020; 1-13.
33. Sudha S, Ramesh P, Kumari CRT, et al. Growth, spectroscopic, HOMO-LUMO energies, MEP, hardness and TG/DTA studies of acid potassium hydrogen fumarate as an efficient nonlinear optical material. J Mol Struct. 2020;1209:1-9.
34. Mary YS, Yalcin G, Mary YS, et al. Spectroscopic, quantum mechanical studies, ligand protein interactions and photovoltaic efficiency modeling of some bioactive benzothiazolinone acetamide analogs. Chem Pap. 2020;1-8.
35. Sheena Mary Y, Ertan-Bolelli T, Thomas R, et al. Quantum mechanical studies of three aromatic halogen-substituted bioactive sulfonamidobenzoxazole compounds with potential light harvesting properties. Polycycl Aromat Compd. 2019;1-17.
36. Guerrab W, Lgaz H, Kansiz S, et al. Synthesis of a novel phenytoin derivative: Crystal structure, Hirshfeld surface analysis and DFT calculations. J Mol Struct. 2020;1205:1-11.
37. Shahab S, Sheikhi M, Filippovich L, et al. Synthesis, geometry optimization, spectroscopic investigations (UV/Vis, excited states, FT-IR) and application of new azomethine dyes. J Mol Struct. 2017;1148:134-49.